JMEPEG (2010) 19:568–571
DOI: 10.1007/s11665-009-9525-4

1059-9495/$19.00

Kinetics of Failure Rate Accumulation and TiNi Shape Memory Effect Alloy Fracture Under Mechanical Cycling

A.B. Bondarev, M.A. Khusainov, G.V. Plastilina, and V.A. Andreev

(Submitted October 29, 2008; in revised form July 8, 2009)

Wire specimens, $d = 0.1$ mm, made of Ti-(50.6-50.8)at.%-Ni alloy were exposed to thermo-mechanical treatment (TMT), thus making the samples straight and providing them with high superelasticity (ε_{se}). It was established that the most effective method of TMT is annealing with deformation at 500 and 300 °C. The optimum mode of treatment was used in the research of mechanical fatigue of alloys with high superelastic properties. Two stages characterizing the alloy behavior under mechanical cycling were found out: failure accumulation and fracture. It was shown that the duration of the cycles is determined by the value of the preset deformation (σ_{set}) in relation to the deformation on the plateau-shaped area. The results of low-cycle fatigue of the alloys under investigation were processed by means of the method of least squares. The equations of prognosis of longetivity at the preset level of deformation are presented.

Keywords heat treating, shaping, superalloys

1. Introduction

Due to the extensive use of SMA materials in different areas of application, one should study their behavior under mechanical cycling in isothermal conditions. It should be noted, however, that stability of superelastic properties depends on the alloy structure and on the level of deforming stresses. In particular, it was shown in Ref 1, 2 that wire drawing and cold rolling harden TiNi alloys. According to Ref 3, TMT serves to form a stable structure with high fatigue resistance. In Ref 4, the authors prove that the fatigue life is connected with the accumulation of plastic deformation in austenite, resulting in fracture. It is true that an incomplete recovery of superelastic deformation with the removal of the load characterizes an irreversible phenomenon, increasing with the subsequent cycles. As a result, the development of residual deformation (ε_r) is possible, then either the process stabilizes at small superelastic deformations, or the material fractures. Consequently, establishing a connection between the structure and the properties of the alloys with superelastic properties is an important issue, and it can increase their working efficiency.

2. Experimental

The research was conducted on samples of wire, $d =$ 1.0 mm, made of Ti-50.8 at.% Ni alloy with the temperature of martensitic transformations: $M_s = (-43)$ °C; $M_f = (-52)$ °C; $T_R = (-22)$ °C; $A_s = (-18)$ °C; $A_f = (-8)$ °C. All specimens were exposed to a two-stage stabilizing treatment under the following conditions:

(I) (1) Heating to 500 °C, time $\tau = 1.0$ min, deformation $\varepsilon = 0.8\%$, cooling on unloading; (2) 300 °C, $\tau = 0.5$ min, $\varepsilon = 0.5\%$.
(II) (1) 500 °C, $\tau = 3.0$ min, $\varepsilon = 0.4\%$; (2) 300 °C, $\tau =$ 0.5 min, $\varepsilon = 0.4\%$.
(III) (1) 500 °C, $\tau = 10$ min, $\varepsilon = 0.75\%$; (2) 300 °C, $\tau =$ 0.5 min, $\varepsilon = 0.6\%$.

After the mentioned types of TMT, the mechanical properties were measured on a tension testing machine FPZ-1.0 (Germany) with the diagrams loading ↔ unloading within the limits of the plateau-shaped area ($\varepsilon = 5\%$). Phase transition of austenite-martensite deformation ($A \rightarrow M_\varepsilon$) occurred on loading, and ($M_\varepsilon \rightarrow A$) on unloading. Table 1 shows the numerical values of the key parameters of hysteresis of the martensitic transformations of the alloys under investigation with superelastic properties; where σ_{ph} = phase yield stress; $\Delta\sigma$ = mechanical hysteresis; ε_r = residual deformation; ε_{se} = superelastic deformation.

As these results indicate, the optimum TMT for the wire samples is regiment III, since the alloy longetivity increases after this kind of treatment. The main difference of this treatment from regiments I and II is that the specimens were subjected to annealing at 500 °C for 10 min. This effect is connected with the stress relaxation in the wire samples, produced by wire drawing. The decrease of the phase yield strength confirms this hypothesis. The small residual deformation of 0.1% at the first cycle is caused by uniformity of texture, for after the second cycle the hysteresis loop closes on unloading (Table 1).

3. Results and Discussion

The wire samples after these procedures become quite straight and possess improved superelastic properties. Similar

A.B. Bondarev and **V.A. Andreev**, Industrial Centre MATEKS Ltd, Moscow, Russia; and **M.A. Khusainov** and **G.V. Plastilina**, Yaroslav the Wise Novgorod State University, Novgorod the Great, Russia. Contact e-mails: Mikhail.khusainov@novsu.ru and andreev@mateks.ru.

results are obtained in Ref 1, but a large mechanical hysteresis prevents this kind of TMT from practical application as a consequence of significant energy losses. The authors of Ref 2 managed to find such modes of treatment that give a narrow flag-shaped hysteresis loop. This effect can be explained by R-phase martensite formation. It is known that R-phase encourages reversibility of the preset deformation. When searching for improved ways of stabilizing the alloy microstructure, one should take into consideration the positive influence of laminar domains, in four variants, twinned relatively to each other on the twinning plane (110) (Ref 5).

Analysis of the kinetics of failure accumulation and fracture of the wire specimens was done using the data obtained from mechanical cycling under double-sided (symmetric) bend at deformation strains of 5%.

Table 1 Functional properties of Ti-50.8at.% Ni alloys after TMT

TMT regiment	σ_{ph}, MPa	$\Delta\sigma$, MPa	ε_r, %	ε_{se}, at the second cycle
I	660	265	0.5	5.0
II	580	225	0.14	5.2
III	510	270	0.1	5.6

The wire specimens were subjected to mechanical cycling at some stages according to the formula $n_i = k_i N_{fr}$; where k_i = coefficient (see Table 2), N_{fr} = a number of cycles before fracture (562 cycles in total), ε = 5%. These data were used for studying the behavior of the failure accumulation and fracture.

Table 2 demonstrates that with an increasing number of cycles the wire samples revert and recover the original shape with the simultaneous growth of the phase yield strength (σ_{ph}). As a result, the superelasticity increases. The evidence of this is the decrease of deformation of incomplete recovery (ε_r) and the increase in superelastic deformation (ε_{se}). Mechanical hysteresis ($\Delta\sigma$) essentially does not change, the width ($\Delta\sigma$) remains the same: 250-260 MPa at the first cycles and 225-230 MPa at the second cycles (Fig. 1).

The results obtained do not fully explain the mechanism responsible for accumulation of the defects of structure and failure of the alloy under mechanical cycling. It is suggested that with the increasing dislocation density alloy strengthens as a consequence of the irreversible defects, impeding the redirection of martensitic crystals and stabilizing of the alloy structure. The power breakdown boosts microcrack generation and development. Upon reaching its critical value, the material fractures. Figure 2 presents experimentally obtained data on longetivity of alloys with superelastic properties.

The results of the experiments were processed statistically using the method described in Ref 5. After dispersion analysis

Table 2 Change in the parameters of hysteresis superelasticity with an increasing number of mechanical cycles

	Number of cycles									
k_i:	k_1 = 0.004		k_2 = 0.05		k_3 = 0.09		k_4 = 0.5		k_5 = 0.95	
	1	2	29	30	51	52	280	281	534	535
Parameters										
ε_r, %	0.5	0.4	0.2	0.1	0.3	0.1	0.2	0.0	0.1	0.0
ε_{se}, %	3.9	3.9	5.2	3.2	6.0	5.6	6.3	6.3	6.7	6.7
σ_{ph}, MPa	500	480	510	480	520	525	540	520	560	540
$\Delta\sigma$, MPa	255	230	265	245	250	225	250	225	255	230

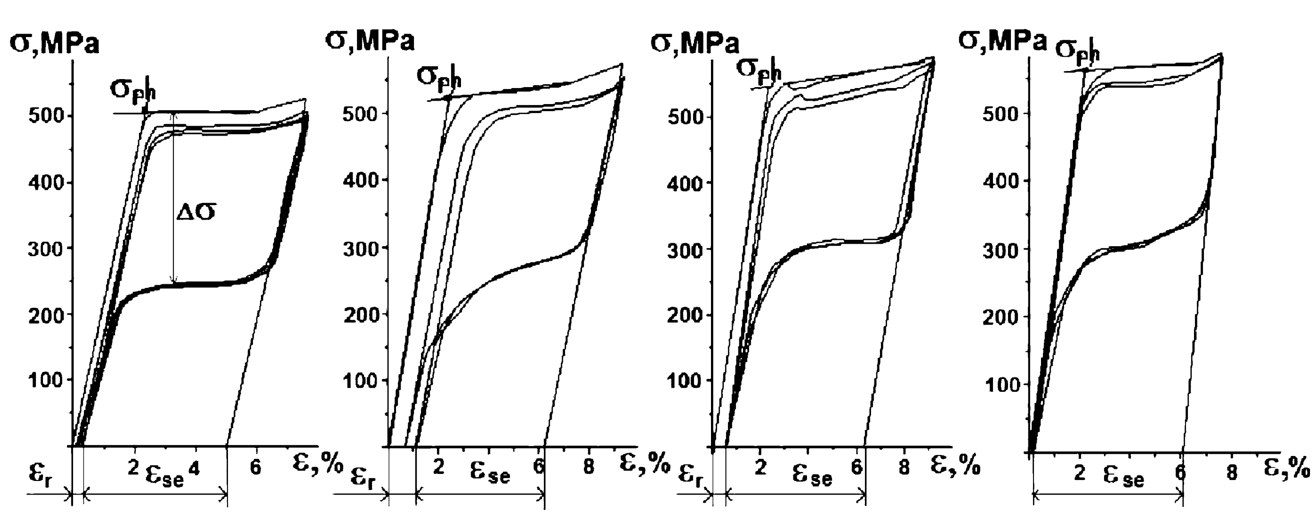

Fig. 1 Diagrams of superelasticity at room temperature. (a) After 30 mechanical cycles under double-sided (symmetric) bend, ε = 5%; (b) 52 cycles; (c) 281 cycles; (d) 535 cycles. At 562 cycles, the sample fractures

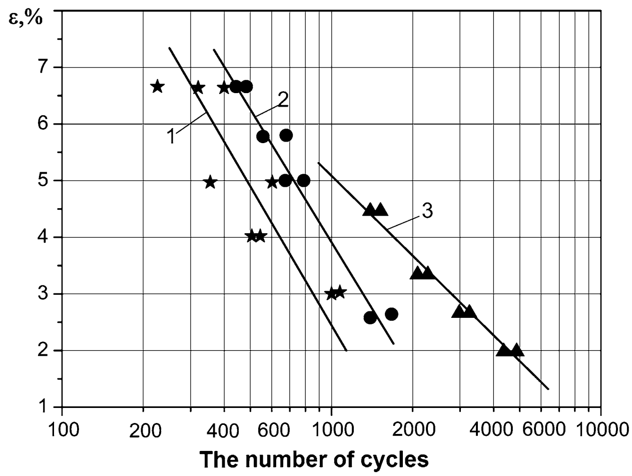

Fig. 2 The dependence of the number of cycles before fracture on the pre-set deformation after TMT, regiment III. (1) alloy Ti-50.65at.% Ni; (2) alloy Ti-50.8at.% Ni; (3) alloy Ti-50.8at.% Ni after electromechanic polishing of the surface

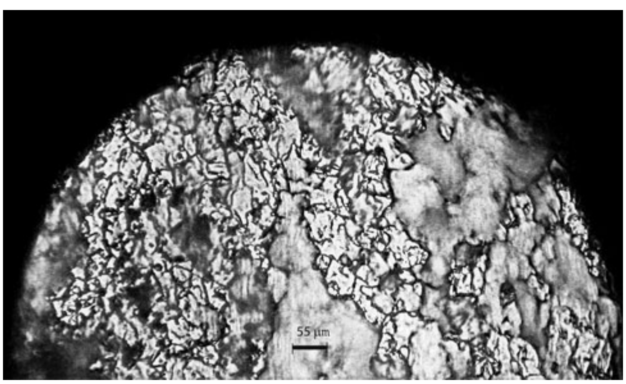

Fig. 3 A typical view of the rupture surface of the specimens after mechanical cycling ×800

of the collected values for the number of cycles to fracture, N_{fr}, for every degree of deformation a regression analysis was done by means of the computer program Microsoft Excel. The most suitable dependence $N_P = f(\sigma)$ proved to be exponential, transformed after into a logarithmic linear form $\lg N_P = a\varepsilon + b$ with the parameters a and b as follows: for Curve 1, $\ln N_{fr} = (-29.67)\ \varepsilon + 7.68$; for Curve 2, $\ln N_{fr} = (-26.22)\varepsilon + 7.9$; and for Curve 3, $\ln N_{fr} = (-39.80)\varepsilon + 9.13$.

The coefficient of determination (R_2) in all experiments was approximately 1 (0.71-0.95), and ($\bar{r}$) was $<10\%$. These estimates of the process gave support to the expectation that regression equations found adequately described the results of the experiments. Thus, they may be used for prognosis of mechanical-cyclical longevity of such types of alloys. The value of (a) in the equation is determined as *tg* of a slope of curve to axis ε, it characterizes structural condition of the alloy; (b) denotes influence of a chemical composition on longetivity.

Fractographic analysis by means of a metallographic microscope ALTAMI MET-3 showed that the failure, irrespective of the level of the pre-set deformation (ε_{set}) or applied stress, follows the type seen in the transcrystalline fracture with

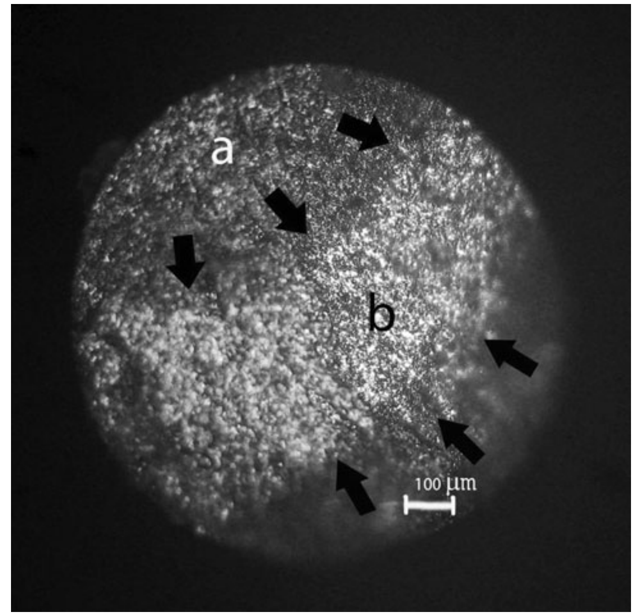

Fig. 4 A typical view of the crack development (a) and the area of the final fracture (b) at small values of pre-set deformation ($\varepsilon_{set} \leq$ 3%) × 100. The arrows show the direction of the crack development

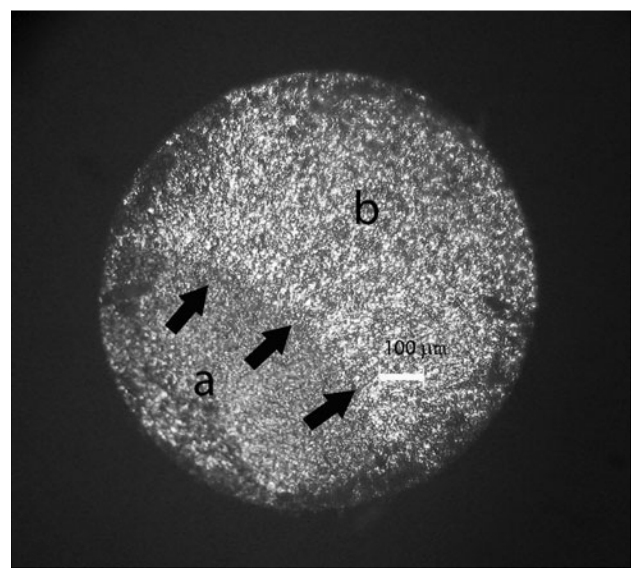

Fig. 5 The area of the crack development (a) and of the final fracture (b) at high values ($\varepsilon_{set} \geq$ 4%) × 100

a small share of local plastic deformation. It is testified by the steps in the cleavage and the shift (Fig. 3), formed as a consequence of the crack crossing the spiral dislocations.

The fracture surface of the wire specimens is mainly perpendicular to its axis. Relatively flat areas of failure can be observed in the fracture. Such failure behavior occurred only in the case of symmetrical (double-sided) cyclic bend. The magnitude of applied stress does not essentially change the view of failure. The difference is only in the ability of branching of the extending crack and in material volume coverage as a consequence of the stresses relaxation in the crack tip. In particular, it can be seen (Fig. 4 and 5) that at small values of pre-set deformation (ε_{set}), the extending crack covers more volume of the metal up to the stage of the final fracture (Fig. 4), than at higher values of ε_{set}.

4. Summary

1. A new mode of wire treatment after drawing was developed, making the wire samples straight and providing them with enhanced superelasticity. The defining principle assumed as a basis of this treatment included deformation at 500 and 300 °C was determined.
2. Kinetics of failure accumulation is shown as a result of functional-mechanical properties of the alloys under consideration after mechanical cycling on the scheme of a symmetrical bend at the preset deformation $\varepsilon = 5\%$. Some interesting peculiarities were noted, namely the continuous alloy strengthening until the loss of structural stability of the material with its subsequent fracture.
3. The fracture mode caused by different levels of deformation under loading was classified. It helped judge the mechanisms controlling crack generation and development.

References

1. A. Heckman and E. Handbogen, Microstructure and Pseudo-Elastic Low-Cycle High Amplitude Fatigue of TiNi. *J. Phys. IV France*, 2003, 112, p 831–834. EDP Sciences, Les Ulis,
2. P. Filip and A.C. Kneissl, Mechanical Properties and Related Substructure of TiNi Shape Memory Alloys, *J. Physique IV*, 1995, **5**, p C8-575–C8-580
3. P. Filip, J. Rusek, and K. Mazanec, Mechanical Behavior of TiNi Shape Memory Alloys, *Z. Metallkunde*, 1991, **82**, p 488–491
4. K.N. Melton and O. Mercier, Fatique of NiTi Thermoelastic Martensite, *Acta Metall.*, 1979, **27**, p 137–144
5. N. Makarova and V. Trofimets, Science, Moskow, Statistics, 2003, 220 p